Journal of Low Temperature Physics (2024) 216:450–457
https://doi.org/10.1007/s10909-024-03179-x

Quasiparticle Cooling, Scattering, and Diffusion Simulations in 1D

Soren Ormseth[1] · Peter Timbie[1] · David Harrison[1] · Robert McDermott[1] · Emily Barrentine[2] · Thomas Stevenson[2] · Eric Switzer[2] · Carrie Volpert[2]

Received: 3 November 2023 / Accepted: 15 June 2024 / Published online: 5 July 2024

Abstract
Kinetic Inductance Detectors (KIDs) are an emerging technology useful for a wide variety of astronomy applications, including the Habitable Exoplanet Imaging Mission (HabEx), the Origins Space Telescope (OST), the Probe of Inflation and Cosmic Origins (PICO), and more. KIDs operate at cryogenic temperatures and can detect photons with high accuracy, sensitivity, and over a wide range of wavelengths. Though many KID models describe their performance well under certain operating conditions, some important pieces of physics related to quasiparticle dynamics are not yet either well understood or integrated into these models and can strongly affect device performance. In this paper we describe our framework for building an extended KID model, present the results of a quasiparticle diffusion simulation that incorporates scattering, cooling and diffusion, and discuss plans for the experimental testing of the model. We also discuss additional features to be added into future models that aim to capture a wide variety of potential scenarios encountered by researchers.

Keywords KIDs · Quasiparticles · Superconductors · Resonators

1 Introduction

Kinetic Inductance Detectors (KIDs) were conceived of in 1999 by Zmuidzinas and Leduc, and by as soon as early 2000, measurements were performed on Nb/SiO/Nb microstrip resonators to verify the feasibility of the concept. Since then, various improvements in design and advances in physical understanding have occurred bringing the technology to a mature state where it is used in a wide variety of (astronomy) applications [1].

Peter Timbie, David Harrison, Robert McDermott, Thomas Stevenson, Eric Switzer and Carrie Volpert have contributed equally to this work.

Extended author information available on the last page of the article

The basic operation of a KID can be understood by a lumped-element circuit model with a variable inductor. A superconducting film contains resonant circuits which are coupled to a microwave readout line. These resonators have some length, intrinsic inductance, capacitance, kinetic inductance, and may be open or short circuited at different ends. Depending on these parameters, a resonant circuit can be given some equivalent lumped-element circuit representation which can be seen to have a resonant frequency [2].

A superconductor has superconducting Cooper pairs, or BCS pairs, along with (non-superconducting) quasiparticles. When a photon is incident on the film there is some probability that there will be an absorption which breaks a Cooper pair into two quasiparticles. In order to break a Cooper pair, the energy of the photon, $h\nu$, must exceed the binding energy per pair, 2Δ, where Δ is the gap energy of the superconductor. The change in the number of Cooper pairs or quasiparticles changes the kinetic inductance of the resonator, and thus changes the frequency and width of the resonance, allowing the incident photon energy or power to be inferred [2].

Going beyond the lumped-element model, though, introduces complications. Quasiparticles can be distributed throughout a resonator at different spatial locations and with different energies. Can we predict the time-varying creation, dissipation, location, and energy of the quasiparticles in a resonator? Given a non-equilibrium time-varying energy-spatial distribution, how does this affect the observed resonator parameters? How do more complicated processes like quasiparticle trapping, phonon trapping, two-level-system (TLS) dynamics, and more, affect this time evolution? We hope to answer some of these questions by developing useful simulations that can be used by researchers to predict KID device performance in a wide variety of situations. In this paper, we present some preliminary results of such simulations, as well as the plans to test and further refine and extend the scope of the model.

2 QP Diffusion, Cooling and Scattering in 1D

We first consider diffusion, quasiparticle-phonon scattering, and quasiparticle-quasiparticle recombination (cooling) in a 1D strip. The 1D diffusion equation with a non-spatially-varying diffusion coefficient is:

$$\frac{\partial u(x,t)}{\partial t} = D\frac{\partial^2 u(x,t)}{\partial x^2}, \tag{1}$$

where $u(x, t)$ is the concentration of the species and D is the diffusion coefficient [3]. Quasiparticles with different energies have different diffusion coefficients. So letting D_0 be the high-energy limit for the diffusion coefficient yields the following energy-dependent diffusion coefficient at an energy E:

$$D_E = D_0\sqrt{1-\left(\frac{\Delta}{E}\right)^2}, \tag{2}$$

where Δ is the superconducting gap energy [4]. Meanwhile, the lifetime for a quasiparticle at energy ϵ to scatter to an energy ϵ' by emitting or absorbing a phonon of energy $\epsilon - \epsilon'$ is given by

$$\Gamma^{s}_{\epsilon\to\epsilon'} = \frac{1}{\tau_{0s}} \int_{\Delta}^{\infty} d\epsilon' \frac{(\epsilon-\epsilon')^2}{(kT_c)^3} \left(1 - \frac{\Delta^2}{\epsilon\epsilon'}\right) \frac{\epsilon'}{\sqrt{\epsilon'^2 - \Delta^2}} \times \frac{1 - f(\epsilon')}{|\exp[-(\epsilon-\epsilon')/kT_p] - 1|}, \tag{3}$$

and the lifetime of a quasiparticle state with energy ϵ to recombine with another quasiparticle of any energy ϵ' is given by

$$\Gamma^{r}_{\epsilon,\epsilon'} = \frac{1}{\tau_{0r}} \int_{\Delta}^{\infty} d\epsilon' \frac{(\epsilon+\epsilon')^2}{(kT_c)^3} \left(1 + \frac{\Delta^2}{\epsilon\epsilon'}\right) \frac{\epsilon' f(\epsilon')}{\sqrt{\epsilon'^2 - \Delta^2}} \times \frac{1}{|\exp[-(\epsilon+\epsilon')/kT_p] - 1|}. \tag{4}$$

Here τ_{0s} and τ_{0r} are the characteristic electron–phonon coupling times, k is the Boltzmann constant, T_c is the critical temperature of the superconductor, $f(E)$ is the occupation probability at energy E, $\rho(E) = E/\sqrt{E^2 - \Delta^2}$ is the normalized density of quasiparticle states, T_p is the temperature of the phonons, and $N_p(E) = 1/|\exp(-E/kT_p) - 1|$ is the thermal equilibrium phonon occupation factor at phonon temperature T_p [5]. Note that $N_p(E)$ approaches the Heaviside step function as $T_p \to 0$.

This expression for the density of states, $\rho(E)$, is derived from BCS theory; however, Dynes has argued that the density of states may need to be broadened. This broadening is well approximated by

$$\rho(E,\theta) = \mathrm{Re}\left\{ \frac{E - i\theta}{[(E - i\theta)^2 - \Delta^2]^{1/2}} \right\}$$

which just results from making the substitution $E \to E - i\theta$ into the original BCS density of states function $\rho(E)$ [1].

2.1 Numerical Simulation

2.1.1 Diffusion

Using the above equations, we simulate the diffusion, cooling, and scattering of quasiparticles in a 1D superconducting strip of length L from time $t = 0$ to $t = T$. To numerically simulate diffusion, the strip is broken into n_x cells where the size of each cell is given by $\Delta x = \frac{L}{n_x}$, finite time steps are given by step size $\Delta t = \frac{T}{n_t}$, and u_i is proportional to the total quasiparticle occupation in the ith cell. Then, we employ the finite volume method. The simplest discrete approximation to Eq. (1) is given by the explicit "forward in time, central in space" (FTCS) method:

$$\frac{u_i^{j+1} - u_i^j}{\Delta t} \approx D \frac{u_{i+1}^j - 2u_i^j + u_{i-1}^j}{\Delta x^2}.$$

The i index refers to the "i-th" location in space, and the j index refers to the "j-th" cell of time. Although the FTCS method is fast, it is only accurate to first-order, and it has the unfortunate numerical stability condition $\Delta t \leq \frac{1}{2}\frac{\Delta x^2}{D}$, meaning that a doubling of the spatial resolution Δx requires a simultaneous reduction in the time-step Δt by a factor of four. Thus, simulating a long time T is unwieldy. One of the most popular methods, therefore, and the method we employ, is the Crank–Nicolson Method [3, 6]. This uses instead the average of the approximations at the points (x_i, t_j) and (x_i, t_{j+1}) :

$$\frac{u_i^{j+1} - u_i^j}{\Delta t} \approx D\frac{(u_{i+1}^{j+1} - 2u_i^{j+1} + u_{i-1}^{j+1}) + (u_{i+1}^j - 2u_i^j + u_{i-1}^j)}{2\Delta x^2}.$$

Or, letting $\alpha = D\frac{\Delta t}{\Delta x^2}$ yields:

$$-\alpha u_{i+1}^{j+1} + 2(1+\alpha)u_i^{j+1} - \alpha u_{i-1}^{j+1} = \alpha u_{i+1}^j + 2(1-\alpha)u_i^j + \alpha u_{i-1}^j. \tag{5}$$

The Crank–Nicolson Method is unconditionally stable regardless of the value of α, and it is accurate to second order in both space and time. The cost of this is that each time step now requires a linear system of equations to be solved. However, given that the matrix involved is tridiagonal, there exist fast algorithms to solve this linear equation. We employ the Thomas algorithm (also known as the tridiagonal matrix algorithm) to do so.

2.1.2 Scattering and Cooling

The quasiparticle lifetimes in Eqs. (3) and (4) are given by integrals over all the possible energy states for a quasiparticle (Δ, ∞). To numerically simulate this we choose some energy range $(\Delta, E_{\max})$ where $E_{\max}$ is sufficiently large and break energy space into cells where the size of each cell is given by $\Delta\epsilon = \frac{E_{\max}}{n_E}$. Then Eqs. (3) and (4) take discrete forms:

$$\Gamma^s_{i\to j} = \sum_j \left[\frac{(\epsilon_i - \epsilon_j)^2}{\tau_{0s}(kT_c)^3}\left(1 - \frac{\Delta^2}{\epsilon_i\epsilon_j}\right)N_p(\epsilon_i - \epsilon_j)\rho(\epsilon_j)\Delta\epsilon\right], \quad \text{and}$$

$$\Gamma^r_{i\to j} = \sum_j \left[\frac{(\epsilon_i + \epsilon_j)^2}{\tau_{0r}(kT_c)^3}\left(1 + \frac{\Delta^2}{\epsilon_i\epsilon_j}\right)N_p(\epsilon_i + \epsilon_j)\right](\Delta\epsilon)\rho(\epsilon_j)f(\epsilon_j).$$

Equivalently,

$$\Gamma^s_{i\to j} = \sum_j G^s_{ij}, \quad \text{and} \quad \Gamma^r_{i\to j} = \sum_j G^r_{ij}n_j,$$

where the G matrices are the terms appearing in brackets:

$$G^s_{ij} = \frac{(\epsilon_i - \epsilon_j)^2}{\tau_{0s}(kT_c)^3}\left(1 - \frac{\Delta^2}{\epsilon_i\epsilon_j}\right)N_p(\epsilon_i - \epsilon_j)\rho(\epsilon_j)\Delta\epsilon, \quad \text{and}$$
$$G^r_{ij} = \frac{(\epsilon_i + \epsilon_j)^2}{\tau_{0r}(kT_c)^3}\left(1 + \frac{\Delta^2}{\epsilon_i\epsilon_j}\right)N_p(\epsilon_i + \epsilon_j),$$

where $n_i \equiv (\Delta\epsilon)\rho(\epsilon_i)f(\epsilon_i)$ [7] is the *quasiparticle* density in the i-th energy bin. We have assumed here a small occupation and so we replace $1 - f(\epsilon') \to 1$ in Eq. (3). Note that N_p again just stands for the thermal equilibrium *phonon* occupation factor; p is not a parameter. The (discretized) equation for the time rate of change in n_i is then

$$\frac{\Delta n_i}{\Delta t} \equiv \frac{n_i^{k+1} - n_i^k}{\Delta t} = \sum_j G^s_{ji} n_j^k - \sum_j G^s_{ij} n_i^k - \sum_j 2G^r_{ij} n_j^k n_i^k \tag{6}$$

Note the factor of 2 here arises from the definition of the recombination rate. If the *recombination* rate is Γ, then the *loss* rate is 2Γ [8].

2.1.3 Diffusion and Scattering/Cooling

Generic diffusion in one dimension has been described, and quasiparticle cooling and scattering have been described in energy space with 0 spatial dimensions. Formally speaking, the time evolution of the 1D system can be described by a master equation in position-energy space. Once discretized, each time step would update the position-energy distribution appropriately. Practically speaking, and for the present purposes, we assume that the diffusion and energy scattering/cooling take place independently. That is, for each time step we simply first loop through every position bin and update the corresponding energy "vector" using the 0 dimensional model, and afterward we loop through each energy bin and update the corresponding spatial "vector" using the Crank-Nicolson scheme with the appropriate energy-dependent diffusion coefficient.

3 Discussion

Figure 1 at the end of the document shows the results of such a simulation for an aluminum (Al) strip with $L = 100\ \mu\text{m}, \tau_{0s} = \tau_{0r} = 400\ \text{ns}, D_0 = 6\ \mu\text{m}^2/\text{ns}, \Delta = 1.7 \times 10^{-4}\text{eV}, T_c = 1.2\ \text{K}, T_p = 0.1\ \text{K}$, and $\theta = 0.001$ Insulated boundary conditions are chosen, and quasiparticles are constantly "injected" at the top end at a rate of $r = 10^{-4}/(\mu\text{m eV ns})$ and an injection energy of $E_{\text{inj}} = 1.9\Delta$.

Note in Fig. 1 the discontinuous line at the injection energy of 1.9Δ. Quasiparticles at any energy E are most likely to scatter to energies close to the gap Δ, *not* to energies near the vicinity of E. Also note that there is very little scattering to energies greater than the injection energy 1.9Δ. The fact that this discontinuous line is clearly visible and diffuses faster than the quasiparticles near Δ shows that the

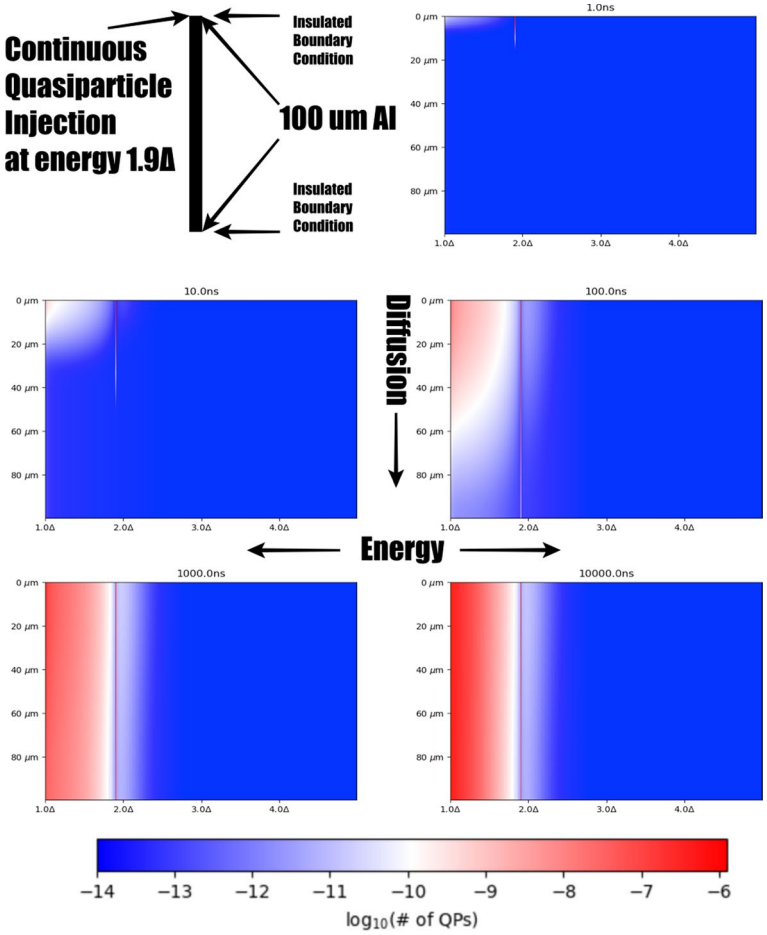

Fig. 1 Simulation Results for 1D strip of aluminum of length 100. Smaller time steps were used to enhance resolution for smaller simulation times. Quasiparticles are injected at the top (as seen in 1.0 ns) at an energy of 1.9Δ and diffuse downward. Parameters: $L = 100\ \mu\text{m}, \tau_{0s} = \tau_{0r} = 400\ \text{ns}, D_0 = 6\ \mu\text{m}^2/\text{ns}, \Delta = 1.7 \times 10^{-4}\text{eV}, T_c = 1.2\ \text{K}, T_p = 0.1\ \text{K},$ and $\theta = 0.001$

diffusion is in some sense happening faster than the scattering and recombination at that energy. A steady state is observed by 10 µs.

The results of this simulation will be tested by fabricating narrow strips of superconducting Al with lengths of 100 µm and 200 µm on a silicon wafer of thickness ∼ 380 µm. Coplanar waveguide (CPW) resonators with characteristic impedances Z_0 near 50Ω have been designed to resonate in the range between 5 GHz and 6 GHz. A given coplanar waveguide consists of a narrow, short (∼ 100 µm) strip of Al connected in series to a much longer quarter wave niobium (Nb) resonator. A Josephson Junction will inject quasiparticles at the end of the Al strip which is not in contact with the Nb. In order to confine the quasiparticles, Nb "guards" with a higher gap

energy than Al of will extend out on all sides for 20 μm. To test the simulation in particular, we will look at how the resonant frequency, bandwidth, and roll-off-noise of the resonators change in response to changing quasiparticle density. The simplest "0-dimensional" test of this will be to compare the total number of quasiparticles to the predicted change in kinetic inductance of the resonators, but we also hope to capture any spatially dependent effects.

In general, the quasiparticle-phonon scattering depends on a phonon occupation function N_p which, in the simulation, we have assumed to be an unchanging equilibrium value for some phonon temperature T_p. However, non-equilibrium quasiparticles when scattering and recombining will emit phonons, and this in turn should change N_p (and make it no longer a thermal equilibrium function). In order to keep N_p as unchanging as possible, the silicon wafer will be coated with titanium (Ti) throughout most of the ground plane. Ti has a lower gap energy than Al, so once a phonon has left the Al it will cool to the Ti gap energy and stay in the Ti. Eventually, we hope to update the simulation model to keep track of the phonon dynamics to generalize to a broader range of physical system.

Based on the results of such testing, we will further refine and add to the model to incorporate more complicated dynamics that have wide applicability. The simulation so far is simple in the sense that it has a constant injection rate of quasiparticles at one end which only diffuse, scatter, and recombine. But we aim to capture the quasiparticles dynamics in a wide variety of 2D structures more generally, and we also aim to understand the specific mechanisms for quasiparticle creation in KIDs which will be used for astronomical surveys.

Data Availability Please email sormseth@wisc.edu for access to Jupyter Notebook simulation and layout to chip design.

Declarations

Conflict of interest The authors declare that they have no Conflict of interest.

References

1. J. Zmuidzinas, Superconducting microresonators: physics and applications. Ann. Rev. Cond. Matter Phys. **3**, 169–214 (2012). https://doi.org/10.1146/annurev-conmatphys-020911-125022
2. P. Day, H. LeDuc, B. Mazin, Others: a broadband superconducting detector suitable for use in large arrays. Nature **425**, 817–821 (2003). https://doi.org/10.1038/nature02037
3. D.S. Gurevich, *Lecture Notes; Numerical Methods for Complex Systems I; Diffusion Equation* (University of Münster, Institute of Theoretical Physics). https://www.uni-muenster.de/Physik.TP/en/teaching/courses/numerical_methods_for_complex_systems_i_ws2016-2017.html (Winter Semester 2016-2017)
4. Y. Dong, Y. Li, W. Zheng, Y. Zhang, Z. Ma, X. Tan, Y. Yu, Measurement of quasiparticle diffusion in a superconducting transmon qubit. Appl. Sci. (2022). https://doi.org/10.3390/app12178461
5. J.M. Martinis, M. Ansmann, J. Aumentado, Energy decay in superconducting Josephson-junction qubits from nonequilibrium quasiparticle excitations. Phys. Rev. Lett. **103**, 097002 (2009). https://doi.org/10.1103/PhysRevLett.103.097002
6. J. Peterson, *Lecture Notes; Crank Nicolson Scheme for the Heat Equation* (Department of Scientific Computing, Florida State University). https://people.sc.fsu.edu/~jpeterson/5-CrankNicolson.pdf

7. M. Lenander, H. Wang, R.C. Bialczak, E. Lucero, M. Mariantoni, M. Neeley, A.D. O'Connell, D. Sank, M. Weides, J. Wenner, T. Yamamoto, Y. Yin, J. Zhao, A.N. Cleland, J.M. Martinis, Measurement of energy decay in superconducting qubits from nonequilibrium quasiparticles. Phys. Rev. B **84**, 024501 (2011). https://doi.org/10.1103/PhysRevB.84.024501
8. J. Wenner, J.M. Martinis, Erratum: Measurement of energy decay in superconducting qubits from nonequilibrium quasiparticles. Phys. Rev. B **84**, 024501 (2011). https://doi.org/10.1103/PhysRevB.84.024501

Authors and Affiliations

Soren Ormseth[1] · Peter Timbie[1] · David Harrison[1] · Robert McDermott[1] · Emily Barrentine[2] · Thomas Stevenson[2] · Eric Switzer[2] · Carrie Volpert[2]

✉ Soren Ormseth
sormseth@wisc.edu

Peter Timbie
pttimbie@wisc.edu

David Harrison
dcharrison@wisc.edu

Robert McDermott
rfmcdermott@wisc.edu

Emily Barrentine
emily.m.barrentine@nasa.gov

Thomas Stevenson
thomas.r.stevenson@nasa.gov

Eric Switzer
eric.r.switzer@nasa.gov

Carrie Volpert
c.g.volpert@nasa.gov

[1] Physics, University of Wisconsin-Madison, 1150 University Avenue, Madison, WI 53706-1302, USA

[2] Goddard Institute for Space Studies, NASA, 8800 Greenbelt Road, Greenbelt, MD 20771-2400, USA